

Synthesis, *in silico* studies and cytotoxicity evaluation of novel 1,3,4-oxadiazole derivatives designed as potential mPGES-1 inhibitors

Gizem ERENŞOY¹ , Kai DING^{2,3} , Chang-Guo ZHAN^{2,3} , Ammar ELMEZAYEN⁴ ,
Kemal YELEKÇİ⁴ , Merve DURACIK⁵ , Özlem BİNGÖL ÖZAKPINAR⁵ ,
İlkay KÜÇÜKGÜZEL^{1*} 

¹ Department of Pharmaceutical Chemistry, Faculty of Pharmacy, Marmara University, Haydarpaşa 34668 İstanbul, Turkey.

² Department of Pharmaceutical Sciences, College of Pharmacy, University of Kentucky, 789 South Limestone Street, Lexington, KY 40536, United States.

³ Center for Pharmaceutical Research and Innovation, College of Pharmacy, University of Kentucky, 789 South Limestone Street, Lexington, KY 40536, United States.

⁴ Department of Bioinformatics and Genetics, Faculty of Engineering and Natural Sciences, Kadir Has University, İstanbul, Turkey.

⁵ Department of Biochemistry, Faculty of Pharmacy, Marmara University, Haydarpaşa 34668 İstanbul, Turkey.

* Corresponding Author. E-mail: ikucukguzel@marmara.edu.tr (İ.K.); Tel. +90-216-414 29 63.

Received: 18 May 2020 / Revised: 24 June 2020 / Accepted: 25 June 2020

ABSTRACT: A series of new 1,3,4-oxadiazole derivatives containing thioether group, has been synthesized to investigate their mPGES-1 inhibitory activities. The synthesized compounds were also evaluated for their anticancer and COX-1/2 inhibitory activities. All compounds were checked for their purity using TLC and HPLC analyses. The melting points, elemental analysis, FT-IR, ¹H-/¹³C-NMR and LR-MS data were utilized for structural characterization. The most potent derivative was 2-[5-[[2-methyl-5-(propan-2-yl)phenoxy]methyl]-1,3,4-oxadiazol-2-yl]sulphonyl]-1-(phenyl)ethan-1-one **3a**, which showed inhibitory activity against mPGES-1 with an IC₅₀ of 4.95 µM. Docking studies with mPGES-1 and COX-1/2 enzymes revealed their affinity and potential binding mechanism for the tested compounds.

KEYWORDS: 1,3,4-Oxadiazoles; thioethers; mPGES-1 inhibition; COX-1/2 inhibition; anticancer activity; molecular docking; ADME prediction.

1. INTRODUCTION

Cyclooxygenase (COX) enzymes are critical macromolecular targets for the management of inflammation, pain and fever. Two major isoforms, COX-1 and COX-2 are structurally similar enzymes, but their regulations are different. While COX-1 is continuously released from many cells under normal physiological conditions, COX-2 is induced by cytokines, growth factors and bacterial endotoxins in case of inflammatory stimuli. These enzymes are also responsible for increased amount of prostaglandins in case of inflammation [1-3]. Prostaglandin E₂ (PGE₂) is the most abundant one among all of them [4] and isomerization of PGE₂ is catalyzed with microsomal prostaglandin synthases (mPGES). PGE₂ is responsible for vascular inflammation and synthesized via mPGES enzymes [5]. Because of side effects of long-term use of COX-1 and COX-2 inhibitors [6, 7] three different microsomal prostaglandin synthases: mPGES-1, mPGES-2 and cPGES (cytosolic) has become newly important target for inflammatory stimuli. Among them mPGES-1 is the most related one to inflammation pathway [8] and it is known that COX-2 and mPGES-1 are induced in response to inflammation [5]. According to earlier reports, mPGES-1 enzyme has also been associated with different diseases such as Alzheimer's, atherosclerosis, rheumatoid arthritis, neuroblastoma and different types of cancer [9].

1,3,4-Oxadiazole is a significant scaffold possessing different biological effects such as anti-inflammatory [10], antitubercular [11], anticancer [12-15]. Additionally, 1,3,4-oxadiazole heterocycle is bioisosteres of ester and amide functional groups [14]. Thioether derivatives have also been shown to have many different biological activities such as anticancer [14, 16-19], antimicrobial [20], anti-inflammatory [21, 22], antiviral properties [23].

How to cite this article: Erensoy G, Ding K, Zhan CG, Elmezayen A, Yelekçi K, Duracık M, Bingöl-Özakpınar Ö, Küçükgülzel İ. Synthesis, *in silico* studies and cytotoxicity evaluation of novel 1,3,4-oxadiazole derivatives designed as potential mPGES-1 inhibitors. J Res Pharm. 2020; 24(4): 436-451.

Carvacrol (5-isopropenyl-2-methylphenol) which is starting compound of our study, is a derivative of monoterpene phenol available from the Labiatae family. Antifungal [24], antimicrobial [25], antioxidant [26] activities have been reported for carvacrol as well as anticancer [27-29], anti-inflammatory activity [30-32].

Figure 1 shows promising recent mPGES-1 inhibitors under investigation. An indole-carboxylic acid derivative, 1-[(4-chlorophenyl)methyl]-3-[(*tert*-butylsulfanyl)-5-(propan-2-yl)-1*H*-indole-2-yl]-2,2-dimethylpropanoic acid MK886, inhibited mPGES-1 *in vitro* in nanomolar range [33].

Various chemical classes of compounds like phenanthrene imidazoles (MF-63) [34], 2,4-biarylimidazol derivatives [35], trisubstituted urea derivatives [36], imidazoquinoline derivatives [37-39], sulfonamide derivatives [40] has been identified as mPGES-1 inhibitors. Natural products obtained from plants also showed anti-inflammatory effect by inhibiting mPGES-1 and/or COX enzymes [9]. The differences between human and murine mPGES-1 enzyme [41] and problems such as strong plasma protein binding and high lipophilicity [8, 42], none of these compounds have been identified as therapeutic agent. The compound LY3023703 has been reported as first one, entered the clinical trial [43]. Recently, Glenmark Pharmaceuticals developed dihydropyrido[4,3-*d*]pyrimidine a compound, which has entered phase I, clinical trial named GRC-27864 (Clinical Trials Identifier: NCT02179645) [44]. Compound **4b**, a 5-arylmethylenebarbituric acid derivative was developed by Chang Guo Zhan's lab as an inhibitor of mPGES-1 enzyme [45].

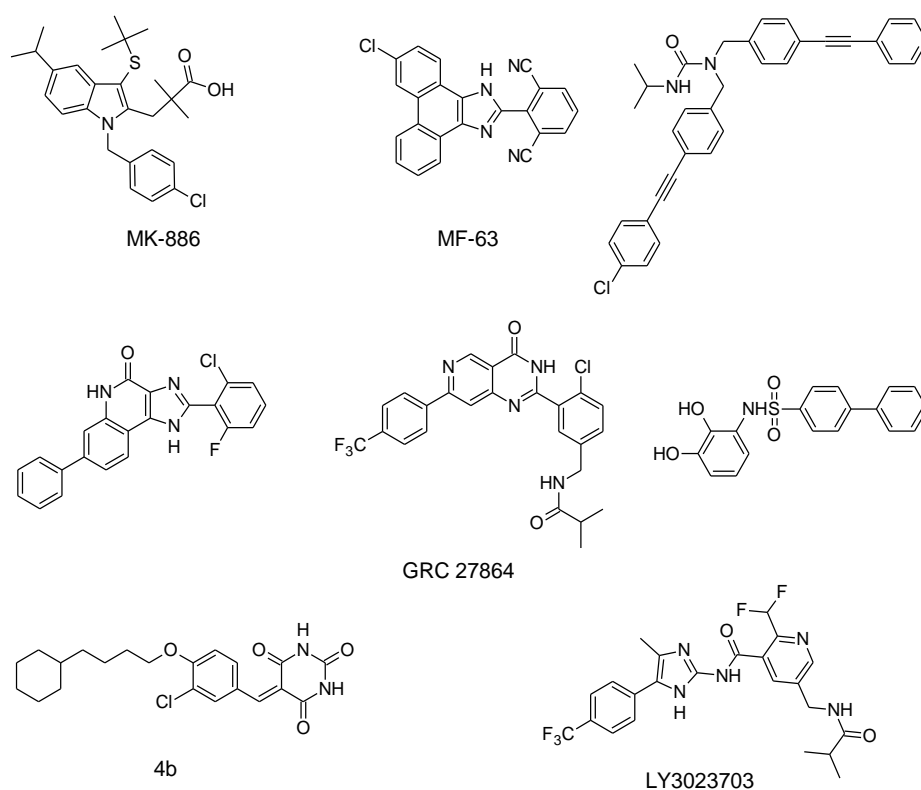


Figure 1. Previously reported mPGES-1 inhibitors.

It is known that the specific inhibition of mPGES-1 reduces the amount of PGE₂ induced by inflammation but does not change the amount of COX-dependent prostanoids. From this point of view, mPGES-1 inhibitors are not expected to cause side effects as in the case of other non-steroidal anti-inflammatory drugs and COX inhibitors [46]. Also, in a recent study, the amount of PGE₂ decreased with mPGES-1 inhibition, whereas PGF_{2 α} and TxB₂ increased. It was revealed that COX-2 inhibition decreases the synthesis of other prostanoids. This demonstrates the selectivity of mPGES-1 rather than COX-2 [47]. Therefore, mPGES-1 has become a very important target for novel anti-inflammatory drug discovery studies.

The compound with new thioether scaffold like our newly synthesized compounds inhibits mPGES-1 enzyme at the concentration of 9.3 nM in cell free assay and 0.7 μ M in human whole blood assay [21]. Although it is known that 1,3,4-oxadiazole derivatives can show anti-inflammatory potency (10), to our knowledge only one compound containing 1,3,4-oxadiazole scaffold showed inhibitory effect against mPGES-1 at 0.42 μ M [48]. Herein this study we report the identification of a new type of inhibitors combining both 1,3,4-oxadiazole and thioether groups through both computational and experimental studies (Figure 2).

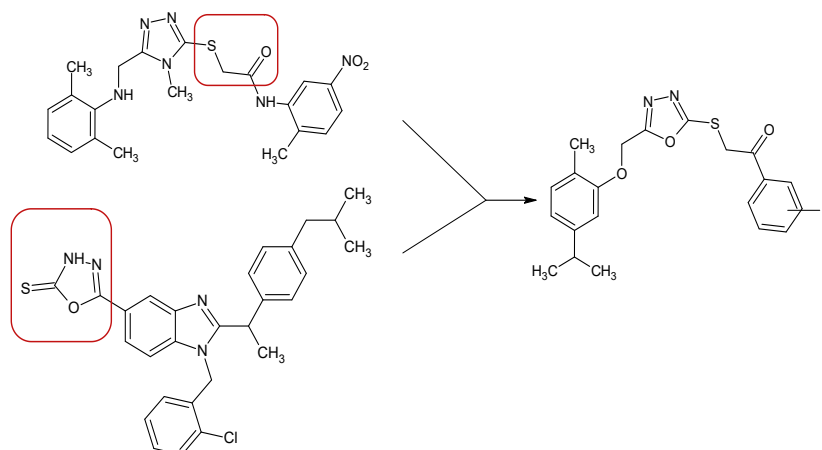


Figure 2. Hybridization of 1,3,4-oxadiazole and thioether groups.

2. RESULTS and DISCUSSION

2.1. Chemistry

Ethyl 2-[2-methyl-5-(propan-2-yl)phenoxy]acetate **1** was prepared by the reaction of carvacrol with ethyl bromoacetate in dry acetone [16,49]. Heating compound **1** with hydrazine hydrate in ethanol gave 2-[2-methyl-5-(propane-2-yl)phenoxy]acetohydrazide **2**. 5-[[2-Methyl-5-(propan-2-yl)phenoxy]methyl]-1,3,4-oxadiazole-2-(3*H*)-thione **3** was obtained by the reaction of compound **2** with KOH and CS₂ in ethanol. As the final step, 2-[5-[[2-methyl-5-(propan-2-yl)phenoxy]methyl]-1,3,4-oxadiazol-2-yl]sulphonyl]-1-(substituted phenyl) ethanone derivatives (**3a-f**) were carried out by the reaction of appropriate α -bromoacetophenone derivatives with compound **3** in the presence of triethylamine (TEA) in acetonitrile [22] (Figure 3).

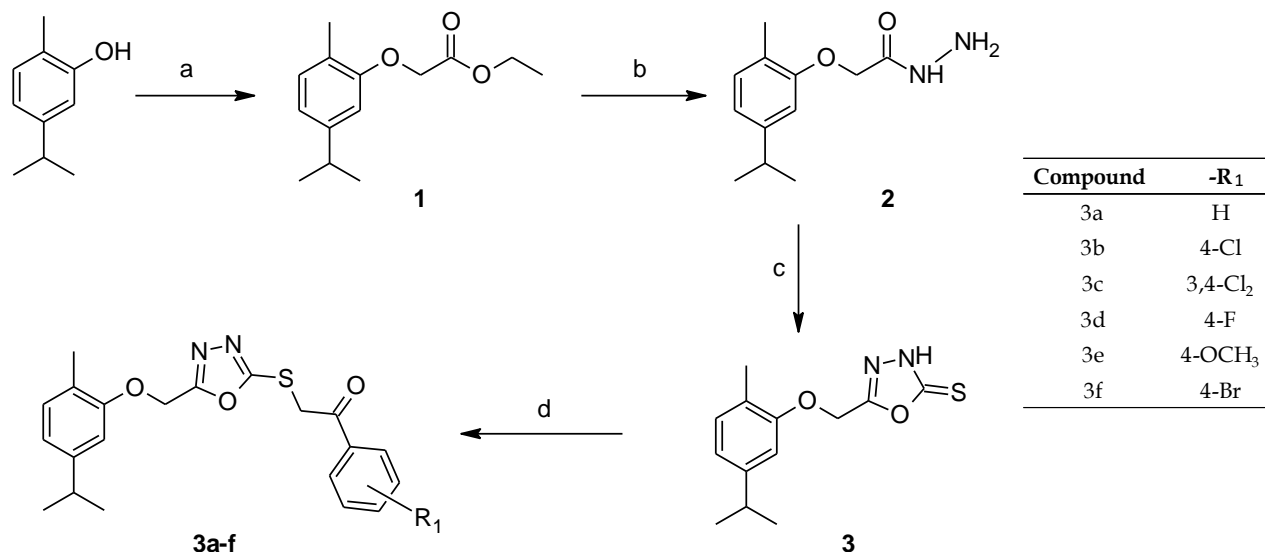


Figure 3. Synthetic route to compounds **3a-f**. Key to reagents: a. BrCH₂COOC₂H₅, K₂CO₃, acetone; b. NH₂NH₂·H₂O, EtOH; c. KOH, CS₂, EtOH, HCl; d. TEA, acetonitrile, α -bromoacetophenone derivatives.

All synthesized compounds were checked for purity using TLC, HPLC-UV/DAD and elemental analysis. All compounds were characterized by their melting points, IR, ¹H-NMR. All ethanone derivatives were (**3a-f**) also characterized with LR-MS spectral data to confirm correct molecular ion peaks corresponding to (M+H)⁺ in positive ionization and (M-H)⁻ in negative ionization modes for each compound. For compounds **3a** and **3b**, HMBC data also recorded.

The C=O stretching band of compound **2**, which was detected at 1666 cm⁻¹ disappeared by the cyclization of this compound to 1,3,4-oxadiazole derivative. The N-H, C=N and C=S stretching bands were observed at 3178, 1610 and 1276 cm⁻¹, respectively. 1,3,4-Oxadiazole-2-thiones may exist in thiole or thione forms. According to the literature, S-H stretching band was observed at 2600-2500 cm⁻¹ values and absence of these bands at IR spectrum of compound **3**, indicated that this compound should exist in thione tautomeric

form [50]. To determine 3D structure of newly synthesized 1,3,4-oxadiazol derivatives, X-Ray crystallography was reported to be carried out and C=S bond length was found consistent with the literature findings [51]. Spectroscopic data also supported that 1,3,4-oxadiazole derivatives may exist in thione form rather than thiole form [52].

The N-H proton of compound **3** was detected at 14.69 ppm in accordance with literature [53] while the S-H proton was reported at 1.6-2.0 ppm [54]. The most important proof of the formation of ketone structure, the C=O stretching bands of compounds **3a-f** which were detected at 1685-1658 cm⁻¹. The disappearance of C=S band and appearance of S-CH₂- protons at 5.07-5.14 ppm are other evidences of this formation.

The HMBC spectra of **3a** and **3b** were taken to identify the interactions between atoms linked by two or three bond distances (Figure 4). Based on the HMBC spectrum of **3a**, the correlations between C16 (192.67 ppm) and H15 (5.14 ppm) and H18 (8.04 ppm) are one of the important ones. The correlations between H15 (5.14 ppm) and C14 (164.84), correlations between H10 (5.37 ppm) and C13 (164.42 ppm), can be seen at Figure 4. The correlations between one of the aromatic protons H18 (8.04 ppm) and C16 (192.67 ppm), C19 (128.91 ppm), C20 (134.46 ppm), H19 (7.57 ppm) and C17 (135.46 ppm), C18 (129.36 ppm), C20 (134.46 ppm), between H3 (6.96 ppm) and C1 (124.03 ppm), C2 (155.79 ppm), C4 (148.08 ppm), C5 (119.77 ppm), between H5 and C1 (124.03 ppm), C2 (155.79 ppm), C3 (111.27 ppm), C6 (130.95 ppm), between H6 and C1 (124.03 ppm), C2 (155.79 ppm), C3 (111.27 ppm), C4 (148.08 ppm) were also indicated in the Figure 4.

The HMBC spectrum of **3b** has similar results like compound **3a**. The correlations between C16 (191.85 ppm) and H15 (5.12 ppm) and H18 (8.06 ppm) were observed. The correlations between H15 (5.12 ppm), C14 (164.77 ppm), the correlations between H10 (5.37 ppm) and C13 (164.45 ppm), the correlations between H18 (8.06 ppm) and C16 (191.85 ppm), C19 (129.59 ppm), C20 (139.43 ppm), the correlations between H19 (7.66 ppm) and C17 (134.15 ppm), C18 (130.82 ppm) and C20 (139.43 ppm) were identified.

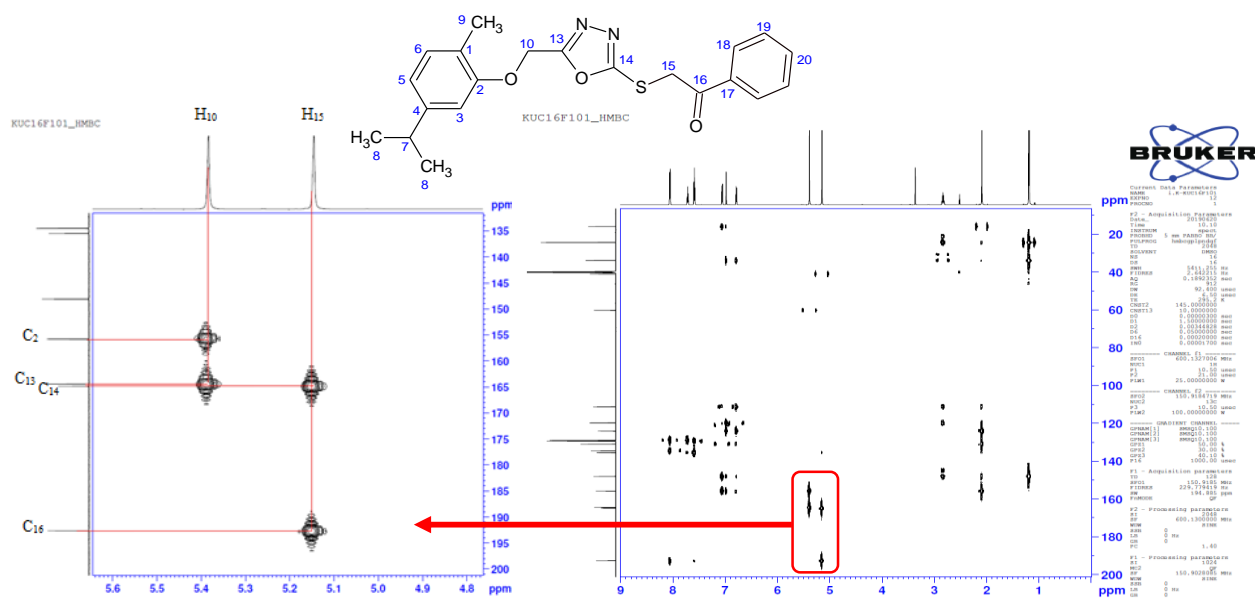


Figure 4. HMBC spectrum of compound **3a** (correlations between 135-200 ppm and 4.8-5.6 ppm).

2.2. Anticancer activity

The anticancer activity of synthesized compounds was evaluated on MCF-7 (breast), A549 (lung), PC-3 (prostate), cervix (HeLa) and K562 (chronic myeloid leukemia) cell lines and murine fibroblast NIH3T3 cell line at 10 μM (Table 1). None of the compounds showed significant inhibition against these cell lines. Therefore, none of the compounds were selected for further testing. The starting compound **3** did not show promising inhibition as well as all thioether derivatives. It is expected that a drug candidate should be cytotoxic to cancer cells but healthy cells. The cytotoxicity of newly synthesized compounds were evaluated against NIH3T3 mouse embryonic fibroblasts. Percent inhibition value range of thioether derivatives appears between 2.01 and 32.61%. As none of the compounds exhibited remarkable inhibition at 10 μM, no further anticancer screening has been made on these compounds.

Table 1. In vitro cytotoxic effects of compounds **3** and **3a-f** against human cancer cell lines and normal cell line.

Compound	Lab ID Code	R ₁	% Proliferation					
			MCF-7	A549	PC-3	HeLa	K562	NIH3T3
3	-	-	103.88	91.83	96.63	72.46	106.14	55.42
3a	KUC16F101	H	90.75	112.60	107.22	96.85	108.40	93.39
3b	KUC16F104	4-Cl	88.14	71.67	81.16	92.43	95.72	97.99
3c	KUC16F106	3,4-Cl ₂	109.35	85.58	122.76	98.13	95.14	91.51
3d	KUC16F109	4-F	107.91	91.50	98.17	103.01	101.18	67.39
3e	KUC16F111	4-OCH ₃	114.62	73.79	80.77	112.62	142.20	87.63
3f	KUC16F115	4-Br	85.95	80.75	80.93	96.17	95.09	102.43
Imatinib	-	-	-	-	-	-	40.46	148.83
Docetaxel	-	-	31.53	22.43	15.56	38.63	-	83.78

2.3. Inhibition of mPGES-1 and COX-1/2 enzymes

Compounds **3a-f** were screened for mPGES-1 inhibitory activity (Table 2). MK-886 and **4b** were used as reference compounds and IC₅₀ values for these compounds were found as 2.58±0.48 and 0.034±0.014 μM, respectively. Compounds that caused an inhibition greater than 70% at 10 μM were further screened at a concentration of 1 μM. IC₅₀ values were determined only for the compounds that showed ≥70% inhibition at 10 μM. Among all of the synthesized compounds, **3a** showed significant inhibitory activity against mPGES-1 enzyme at concentration at an IC₅₀ value of 4.95±2.07 μM. Compound **3a** were determined as a lead compound with its inhibitory potential comparable to the reference compound MK-886 which was demonstrated bioactive mPGES-1 inhibitor [46]. It was interesting that, this unique compound has no substitution at R₁ position and substitution at this location resulted in the loss of activity.

Since both mPGES-1 and COX enzymes have similar membrane embedded configuration [5] and they are both macromolecular targets for inhibition of PGE₂ synthesis, inhibition assay was carried out for COX enzymes too. As a next step for compound **3a**, which showed remarkable inhibition against mPGES-1, we intended to find out whether it has significant inhibitory activity against either COX-1 or COX-2. Inhibition potency of compound **3a** were determined at 100 μM and found as 58.86 and 83.26 μM values for COX-1 and COX-2, respectively. Although this compound had an inhibitory potency at high concentration, this inhibition was not found significantly selective.

Table 2. mPGES-1 inhibition results for **3a-f**.

Compound	Lab ID Code	R ₁	mPGES-1 % inhibition at 10 μM ^a	mPGES-1 IC ₅₀ (μM) ^b	COX-1 % inhibition at 100 μM	COX-2 % inhibition at 100 μM
3a	KUC16F101	H	78±7.6	4.95±2.07	58.86	83.26
3b	KUC16F104	4-Cl	40.4±4.9	-	-	-
3c	KUC16F106	3,4-Cl ₂	6.5±0.2	-	-	-
3d	KUC16F109	4-F	28±2.5	-	-	-
3e	KUC16F111	4-OCH ₃	23±2.1	-	-	-
3f	KUC16F115	4-Br	30±7.3	-	-	-
MK-886 ^c				2.58±0.48		
4b ^c				0.034±0.014		

^aData are expressed as means ± SD of single determinations obtained in triplicate.

^bIC₅₀ values were determined only for the compounds that showed ≥70% inhibition at 10 μM. Data are expressed as means ± SD of single determinations obtained in triplicate.

^cCompounds MK-886 and **4b** were used as reference compounds for the determination of IC₅₀ values. MK-886 is a well-recognized inhibitor against mPGES-1 and **4b** is the inhibitor developed by Chang Guo Zhan's lab [45]. Structures of MK-886 and compound **4b** were given in Figure 1.

2.4. In silico docking studies

Computer-assisted molecular modelling techniques have been used to estimate the possible inhibitory activities and mechanism of binding to COX enzymes and mPGES-1 enzyme of the synthesized compounds [55, 56]. Binding energy was obtained from the docking studies of the compounds **3a–f** by using Autodock4.2. [57]. The results were given in Table 3. Compound **3b** showed slightly higher binding affinity than that of others for mPGES-1 with a predicted binding energy value of -6.61 kcal/mol, and an estimated constant inhibition value of 14.18 μ M. Compound **3b** were found to be interacted with glutathione by a halogen interaction. Other interactions were found including hydrogen bond, π -lone pair, alkyl and various van der Waals interactions (Figure 5 (a)). Especially halogen substitution at R₁ position have been observed to increase calculating binding affinity, probably by providing further halogen interactions by GSH and TYR residues.

In addition, Compound **3b** displayed the highest binding affinity for COX-1 with a predicted binding energy value of -11 kcal/mol, and an estimated constant inhibition value of 8.68 nM. Compound **3b** displayed two H-bonds, π - σ bond, π -Sulfur, alkyl and many van der Waals interactions (Figure 5 (b)). Lastly, compound **3c** had the highest binding affinity for COX-2 with a calculated binding energy value of -11.54 kcal/mol, and an estimated constant inhibition value of 3.49 nM. Compound **3c** showed the highest number of hydrophobic (alkyl) and hydrogen bonds interactions which contributed to the highest affinity and lowest binding energy (-11.54 kcal/mol) among all docked compounds. Also, compound **3c** depicted amide- π and multiple van der Waals interactions (Figure 5 (c)). Most of the interactions within these complexes were π -alkyl, π -sulfur and hydrogen bonds.

Table 3. Docking results of compounds **3a–f**.

Compound	R ₁	PGES-1		COX-1		COX-2	
		ΔG ^a	K _i (μ M) ^b	ΔG	K _i (nM)	ΔG	K _i (nM)
3a	H	-6.21	28.14	-10.36	25.53	-11.32	5.02
3b	4-Cl	-6.61	14.18	-11.00	8.68	-11.02	8.41
3c	3,4-Cl ₂	-6.52	16.62	-10.38	24.79	-11.54	3.49
3d	4-F	-6.09	34.38	-10.19	33.65	-10.34	26.38
3e	4-OCH ₃	-5.95	43.39	-9.79	66.37	-10.81	11.86
3f	4-Br	-6.55	15.86	-10.85	11.14	-11.28	5.40

^a Binding affinity (kcal/mol).

^b Inhibition constant.

2.5. In silico prediction of potential ADME and drug-like properties

ADME properties were calculated using SwissADME online tool program [58] and the results were given in Table 4. Log P is an important physicochemical property for drug discovery and should be <5 due to Lipinski's rule of five. Results showed that all compounds showed compatibility with the acceptable criteria except **3c**, with a log P value slightly higher than 5. Solubility is another important property for drug candidate in order to maintain oral administration and absorption and expressed as Log S. Polar surface area (PSA) and topological polar surface area (TPSA) are important criteria for crossing biological barriers such as blood brain barrier and the value should be smaller than 140 Å. In order to achieve a flexible molecule number of rotatable bands should be smaller than 10. Estimated intestinal absorption calculated with this formula: %ABS= 109-(0.345 × TPSA) according to literature [59].

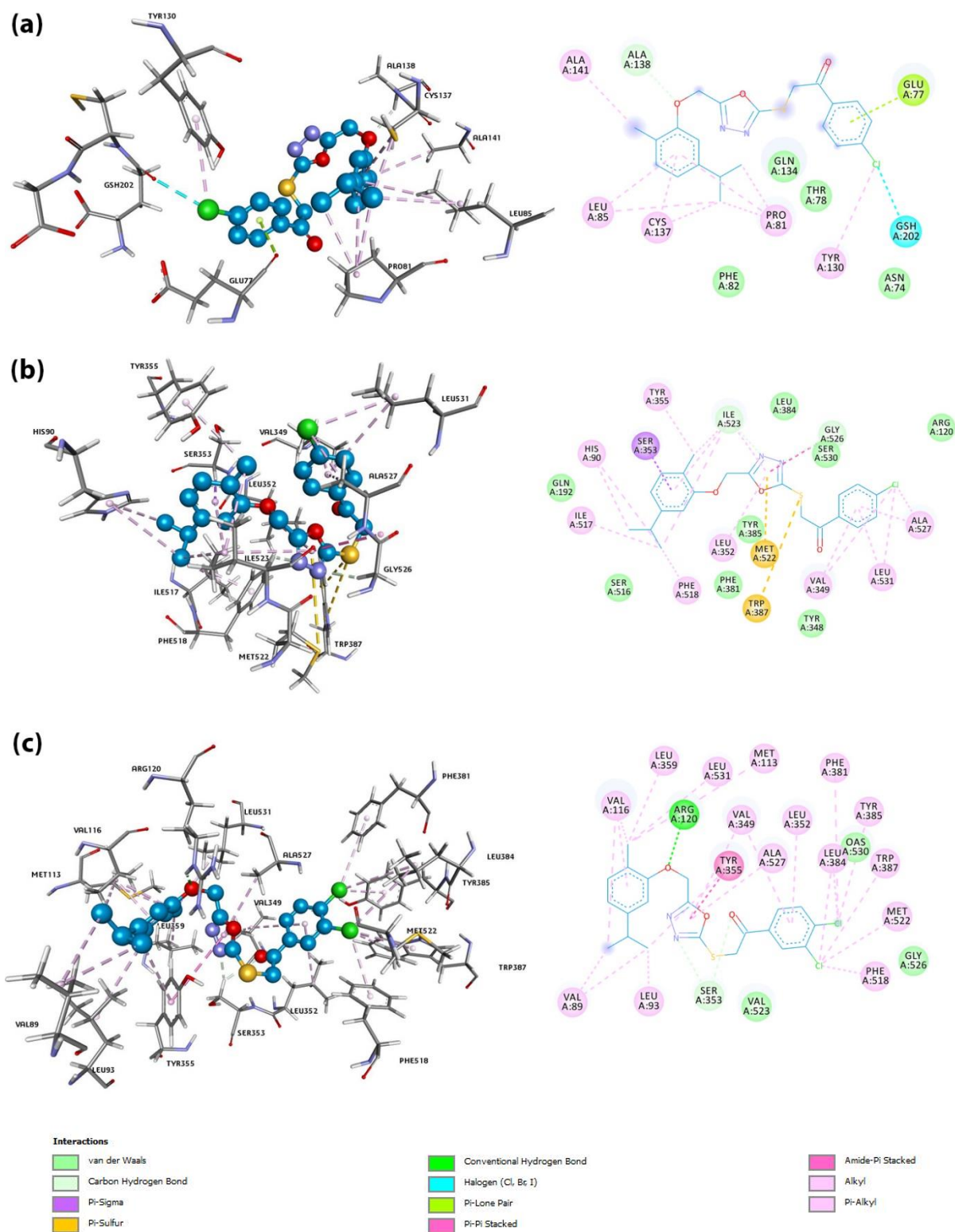


Figure 5. 3D and 2D pictures of the compound **3b** in the active site of mPGES-1 enzyme (a), **3b** complexed with the active site of COX-1 (b) and compound **3c** bound to the binding site of COX-2 (c).

All compounds pass the Lipinski's Rule of 5. Water solubility is an important factor for the drug development. Water solubility value of our compounds are poor (log S value between -7.76 and -8.83). The absorption percent of all thioether derivatives are 77.77% except compound **3e** (74.59%) and this is an indication of acceptable bioavailability by oral route (>50%). Topological polar surface area is the surface of polar atoms ranging between 90.52 and 99.75 for all compounds which indicates low blood-brain barrier penetration, therefore CNS based side effects could not be anticipated. All the tested compounds having less than 10 rotatable bonds which leads to low conformational flexibility. Molar refractivity index is less than 130 for all compounds (106.26-113.96). P-glycoprotein (P-gp) is an ATP-dependent transmembrane protein and have a role in drug transportation. It has excessively found in tumor cells and caused to multi drug resistance. It also can be found in healthy tissues such as liver, kidney, small intestine, colon, brain, heart, peripheral nerves as well as blood-brain and blood-testicular barrier. In the tissues that play a role in ADME properties such as small intestine, central nervous system, liver and kidney, the P-gp expression was found high and that causes to changes pharmacokinetics-toxicokinetics of the substrates of P-gp [60, 61]. The results obtained showed that none of our compounds are a substrate for P-gp. All of compounds are predicted as inhibitors of CYP2C19, CYP2C9, CYP3A4 and as a non-inhibitor for CYP2D6. In Figure 5, the prediction of intestinal absorption and blood-brain barrier penetration is given in the form of *boiled egg model*. In this model, the yellow area indicates well penetration for brain and intestinal absorption. The white area indicates intestinal absorption and lastly grey area indicates poor intestinal absorption [62]. None of our compounds located in the blood-brain barrier penetration area. But all our compounds located in white area which associated with potential intestinal absorption. All synthesized compounds have similar bioavailability score (0.55).

In conclusion these drug-likeness results indicated that, the 1,3,4-oxadiazole-thioether derivatives show good potential for their pharmacokinetic properties, but no blood-brain barrier penetration. All the predicted parameters are within the range of accepted values. However, further optimization needs to continue on prospective compounds, in order to achieve better ADME properties such as solubility.

Table 4. Predicted ADME properties of compounds **3a-f**.

ADME Properties ^a	Compounds					
	3a	3b	3c	3d	3e	3f
MW≤500	382.48	416.92	451.37	400.47	412.50	461.37
CLP<5	4.36	4.90	5.39	4.70	4.43	4.99
logS≥-4	-7.66	-8.24	-8.83	-7.92	-7.76	-8.44
RB≤10	8	8	8	8	9	8
HD≤5	0	0	0	0	0	0
HA≤10	5	5	5	6	6	5
MR 40-130	106.26	111.27	116.28	106.22	112.75	113.96
%ABS	77.77	77.77	77.77	77.77	74.59	77.77
TPSA≤140 Å	90.52	90.52	90.52	90.52	99.75	90.52
GI absorption	High	High	High	High	High	High
P-gp substrate	No	No	No	No	No	No
BBB penetration	No	No	No	No	No	No
Skin permeation (Log Kp)	-5.08	-4.85	-4.62	-5.12	-5.29	-5.07
CYP1A2 inhibitor	Yes	Yes	No	Yes	Yes	Yes
CYP2C9 inhibitor	Yes	Yes	Yes	Yes	Yes	Yes
CYP2C19 inhibitor	Yes	Yes	Yes	Yes	Yes	Yes
CYP2D6 inhibitor	No	No	No	No	No	No
CYP3A4 inhibitor	Yes	Yes	Yes	Yes	Yes	Yes
Bioavailability score	0.55	0.55	0.55	0.55	0.55	0.55

^a Parameter calculated using SwissADME (<http://www.swissadme.ch>).

MW: molecular weight, CLP: cLOGP, logS: solubility, RB: number of rotatable bonds, HD: number of hydrogen donors, HA: number of hydrogen acceptors, MR: molar refractivity, TPSA: topological polar surface area.

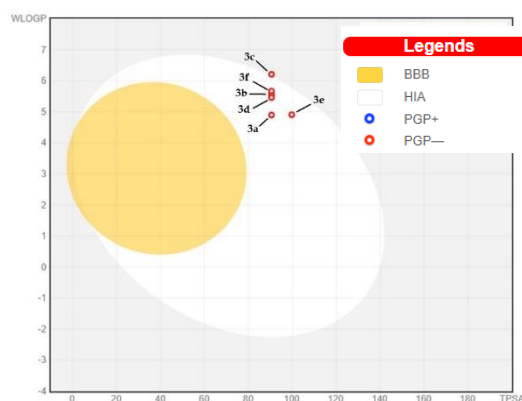


Figure 5. Boiled-egg prediction chart of compounds 3a-f.

3. CONCLUSION

Despite COXs enzymes are important target for the prevention of inflammation, long term use of COXs inhibitors can cause several side effects. mPGES-1 is a potential target in order to inhibit PGE₂ synthesis in inflammatory stimuli and its inhibition also related with other diseases such as cancer. In this study we described the synthesis of six new 2-aryloxymethyl-1,3,4-oxadiazole derivatives as potential inhibitors of mPGES-1 enzyme. Compound 3a was identified as the most potent agent against this enzyme with IC₅₀ value of 4.95 μM. This compound also showed inhibition against COX-2 enzyme greater than 82%. According to docking studies of compound 3b, chlorine substituent at R₁ position estimated slightly higher binding affinity than compound 3a to mPGES-1 enzyme. It can be observed from 2D picture of compound 3b, most of the interactions occurred between the carvacrol-based part of the compound and mPGES-1 enzyme active site. Another pi-lone pair interaction occurred between the second phenyl ring of the compound and enzyme active site. The reason why there is no reliable correlation between mPGES-1 inhibitory activities (percent inhibitions) and the docking scores indicates that there might be other factors except direct interactions of compounds 3a-f with enzyme active site. These factors can be related to poor solubility of chlorinated and brominated derivatives and potential steric effects caused by these substituents. It has been observed that the carvacrol structure is important for interaction with the enzyme. Therefore, future studies on novel carvacrol derivatives are being followed these steps.

4. MATERIALS AND METHODS

4.1. Chemicals and instruments

All solvents and reagents were obtained from commercial sources and used without further purification. The purity of the compounds was confirmed by the thin-layer chromatography (TLC) performed on Merck silica gel 60 F254 aluminium sheets (Merck, Darmstadt, Germany), using developing systems: S1: chloroform/methanol/acetic acid (8:2:400 μL v/v/v), S2: petroleum ether/ethyl acetate (5:5 v/v), S3: petroleum ether/ethyl acetate (7:3 v/v). Spots were detected under UV light at 254 nm. All melting points were determined using Thermo Scientific IA9300 basic model point apparatus and are uncorrected. Elemental analyses were obtained using Leco CHNS-932 and are consistent with the assigned structures. Infrared spectra (IR) were recorded on a Shimadzu FT-IR 8400s and data is expressed in wavenumbers (cm⁻¹). NMR spectra were recorded on Bruker AVANCE DPX 300 MHz for ¹H NMR and 150 MHz ¹³C NMR. The chemical shifts were expressed in ppm (parts per million) downfield from tetramethylsilane (TMS) using DMSO-d₆ as solvent. The high-pressure liquid chromatographic system consists of a Shimadzu LC-20AT series instrument equipped with quaternary solvent delivery system and a model SPD-M20A PDA detector. A Rheodyne syringe loading sample injector with 50 μL sample loop was used for the injection of the analytes. Chromatographic data were collected and processed using Shimadzu LabSolutions software. The separation was performed at ambient temperature by using reversed phase GL Sciences Inertsil ODS-3 (4.6×250 mm, 5μm) column. All experiments were performed in isocratic mode. The mobile phase was prepared by mixing acetonitrile and water (7:3, v/v) and filtered through a 0.45 mm pore filter and subsequently degassed by ultrasonication, prior to use. Solvent delivery was employed at a flow rate of 1 mL/min. Detection of the analytes was carried out at 254 nm. SMILES codes of the compounds were generated from the structures using the ACD/ChemSketch version 12.0 molecular editor [63] and then physicochemical properties were calculated by using SwissADME calculation software [58].

4.2. Chemistry

4.2.1. Synthesis of ethyl-2-[2-methyl-5-(propan-2-yl)phenoxy]acetate (1)

Carvacrol (0.06 mol) and anhydrous potassium carbonate (0.09 mol) were dissolved in dry acetone and heated under reflux for 4 hours. Upon cooling temperature, followed by dropwise addition of ethyl bromoacetate (0.063 mol) for 1 hour, refluxing continued for another 8 hours. The excess solvent was removed, and crushed ice added to deposit. The mixture was stirred for half an hour and extracted with diethyl ether. The organic layer was washed with water and dried with Na₂SO₄. The solvent was recovered under vacuum and yellowish oil obtained. This compound was used in the next step without purification [16, 49]. HPLC t_R (min): 13.92, TLC R_f: 0.74 (S1) yield 80%. IR cm⁻¹: 1760 (C=O), 1197 (C-O-C). ¹H NMR (300 MHz, DMSO-d₆): δ: 1.15 (d, 6H, J=6.9 Hz, -CH(CH₃)₂); 1.21 (t, 3H, J=2.4 Hz, -CH₂-CH₃), 2.14 (s, 3H, Ar-CH₃); 2.80 (m, 1H, -CH(CH₃)₂); 4.17 (q, 2H, -CH₂-CH₃); 4.78 (s, 2H, -O-CH₂-); 6.68 (s, 1H, Ar-H), 6.73 (d, 1H, J=7.8 Hz, Ar-H); 7.04 (d, 1H, J=7.8 Hz, Ar-H).

4.2.2. Synthesis of 2-[2-methyl-5-(propan-2-yl)phenoxy]acetohydrazide (2)

Compound 1 (0.03 mol) and hydrazine hydrate (0.06 mol) in 20 mL ethanol refluxed for 2 hours. Progress of reaction was monitored with TLC. Then the solution was cooled, filtered, dried and recrystallized from ethanol: water mixture [49]. HPLC t_R (min): 4.38, M.p: 128-130 °C, TLC R_f: 0.29 (S1), yield 73%. IR cm⁻¹: 3309 and 3200 (N-H str), 1666 (C=O), ¹H NMR (300 MHz, DMSO-d₆): δ: 1.17 (d, 6H, J=6.9 Hz, -CH(CH₃)₂); 2.14 (s, 3H, Ar-CH₃); 2.80 (m, 1H, -CH(CH₃)₂); 4.34 (s, 2H, -NH₂-); 4.48 (s, 2H, -O-CH₂-); 6.78 (m, 2H, Ar-H); 7.04 (d, 1H, J=9 Hz, Ar-H); 9.20 (s, 1H, CO-NH-). Anal. Calcd. for C₁₂H₁₈N₂O₂: C, 64.84; H, 8.16; N, 12.60. Found: C, 63.34; H, 7.49; N, 12.35.

4.2.3. Synthesis of 5-[[2-Methyl-5-(propan-2-yl)phenoxy]methyl]-1,3,4-oxadiazole-2-(3H)-thione (3)

Compound 2 (0.01 mol) and KOH (0.01 mol) were dissolved in 40 mL absolute ethanol and 0.02 mol CS₂ was added to this solution and refluxed for 4 hours. After reaction completed the solution was cooled to the room temperature and diluted with iced water and neutralized with 10% HCl. The precipitated compound filtered, dried and recrystallized from petroleum ether [64]. HPLC t_R (min): 6.84, M.p: 136-138 °C, TLC R_f: 0.46 (S2), yield 56%. IR cm⁻¹: 3178 (N-H str), 1610 (C=N), 1276 (C=S). ¹H NMR (300 MHz, DMSO-d₆): δ: 1.19 (d, 6H, J=6.9 Hz, -CH(CH₃)₂); 2.12 (s, 3H, Ar-CH₃); 2.76-2.90 (m, 1H, -CH(CH₃)₂); 5.26 (s, 2H, -O-CH₂-); 6.80 (d, 1H, J=6.7 Hz, Ar-H); 6.96 (s, 1H, Ar-H); 7.07 (d, 1H, J=7.2 Hz, Ar-H); 14.69 (s, 1H, N-H). Anal. Calcd. for C₁₃H₁₆N₂O₂S: C, 59.07; H, 6.10; N, 10.60. Found: C, 59.25; H, 6.43; N, 10.13.

4.2.4. General synthesis of compounds 3a-f

An equimolar mixture of compound 3 and substituted phenacyl bromide (0.01 mol) and TEA (0.012 mol) in acetonitrile (50 mL) was heated under reflux for 4–8 h. The reaction mixture was evaporated to dryness. The residue was crystallized from aqueous ethanol affording the pure products [22].

2-[5-[[2-Methyl-5-(propan-2-yl)phenoxy]methyl]-1,3,4-oxadiazol-2-yl]sulphonyl]-1-(phenyl)ethan-1-one (3a): It was obtained as a light yellow solid. HPLC t_R (min): 18.05, M.p: 99-101 °C, TLC R_f: 0.77(S3), yield 69%. IR cm⁻¹: 3061 (Ar C-H str), 1680 (C=O), 1591 (C=N str), 1128 (C-O-C), 684 (C-S-C). ¹H NMR (300 MHz, DMSO-d₆): δ: 1.17 (d, 6H, J=6.9 Hz, -CH(CH₃)₂); 2.07 (s, 3H, Ar-CH₃); 2.77-2.87 (m, 1H, -CH(CH₃)₂); 5.14 (s, 2H, -S-CH₂-); 5.37 (s, 2H, -O-CH₂-); 6.76 (dd, 1H, J=7.5 Hz, J=1.2 Hz, Ar-H); 6.96 (d, 1H, J=1.2 Hz, Ar-H); 7.05 (d, 1H, J=7.8 Hz, Ar-H); 7.57 (t, 1H, J=7.5 Hz, J=1.5 Hz, Ar-H); 8.04 (dd, 1H, J=7.5 Hz, J=1.5 Hz, Ar-H). ¹³C-NMR (150 MHz, DMSO-d₆): δ: 15.89, 24.32, 33.82, 41.01, 60.19, 111.27, 119.77, 124.03, 128.91, 129.36, 130.95, 134.46, 135.46, 148.04, 155.79, 164.42 (oxadiazole C5), 164.84 (oxadiazole C2), 192.67 (C=O). LR-MS (m/z): calculated for (M+H)⁺: 383.142, found: 383, calculated for (M-H)⁻: 381.142, found: 381. Anal. Calcd. for C₂₁H₂₂N₂O₃S. ½ H₂O: C, 64.43; H, 5.92; N, 7.16; S, 8.19. Found: C, 64.75; H, 5.93; N, 7.29; S, 9.09.

2-[5-[[2-Methyl-5-(propan-2-yl)phenoxy]methyl]-1,3,4-oxadiazol-2-yl]sulphonyl]-1-(4-chlorophenyl)ethan-1-one (3b): It was obtained as a white solid. HPLC t_R (min): 24.69, M.p: 137-140 °C, TLC R_f: 0.55 (S3), yield 46%. IR cm⁻¹: 3100 and 3050 (Ar C-H str), 1671 (C=O), 1586 (C=N str), 1121 (C-O-C), 688 (C-S-C). ¹H NMR (300 MHz, DMSO-d₆): δ: 1.17 (d, 6H, J=6.9 Hz, -CH(CH₃)₂); 2.07 (s, 3H, Ar-CH₃); 2.77-2.86 (m, 1H, -CH(CH₃)₂); 5.12 (s, 2H, -S-CH₂-); 5.37 (s, 2H, -O-CH₂-); 6.77 (dd, 1H, J=7.5 Hz, J=1.5 Hz, Ar-H); 6.96 (s, 1H, Ar-H); 7.04 (d, 1H, J=7.5 Hz, Ar-H); 7.66 (dd, 2H, J=6.9 Hz, J=2.1 Hz, Ar-H); 8.06 (dd, 2H, J=8.7 Hz, J=2.1 Hz, Ar-H). ¹³C-NMR (150 MHz, DMSO-d₆): δ: 15.91, 24.33, 33.83, 40.88, 60.11, 111.22, 119.75, 124.00, 129.59, 130.82, 130.86, 134.15, 139.43, 148.07,

155.77, 164.45 (oxadiazole C5), 164.77 (oxadiazole C2), 191.85 (C=O). LR-MS (m/z): calculated for (M+H)⁺: 417.103, found: 417, calculated for (M-H)⁻: 415.089, found: 415. Anal. Calcd. for C₂₁H₂₁ClN₂O₃S: C, 60.50; H, 5.08; N, 6.72; S, 7.69. Found: C, 60.60; H, 5.06; N, 6.66; S, 7.92.

2-[5-[[2-Methyl-5-(propan-2-yl)phenoxy]methyl]-1,3,4-oxadiazol-2-yl]sulphonyl]-1-(3,4-dichlorophenyl)ethan-1-one (**3c**): It was obtained as a yellow solid. HPLC t_R (min): 33.12, M.p: 111-113 °C, TLC R_f: 0.76(S3), yield 37%. IR cm⁻¹: 3086 and 3070 (Ar C-H str), 1685 (C=O), 1581 (C=N str), 1170 (C-O-C), 703 (C-S-C). ¹H NMR (300 MHz, DMSO-d₆): δ: 1.17 (d, 6H, J=6.9 Hz, -CH(CH₃)₂); 2.07 (s, 3H, Ar-CH₃); 2.77-2.86 (m, 1H, -CH(CH₃)₂); 5.13 (s, 2H, -S-CH₂-); 5.38 (s, 2H, -O-CH₂-); 6.77 (dd, 1H, J=7.5 Hz, J=1.5 Hz, Ar-H); 6.96 (s, 1H, Ar-H); 7.04 (d, 1H, J=7.5 Hz, Ar-H); 7.87 (d, 1H, J=8.7 Hz, Ar-H); 7.99 (dd, 1H, J=8.4 Hz, J=2.1 Hz, Ar-H); 8.27 (d, 1H, J=2.1 Hz, Ar-H). LR-MS (m/z): calculated for (M+H)⁺: 451.064, found: 451, calculated for (M-H)⁻: 449.050, found: 449. Anal. Calcd. for C₂₁H₂₀Cl₂N₂O₃S: C, 55.88; H, 4.47; N, 6.21; S, 7.10. Found: C, 55.54; H, 4.45; N, 6.24; S, 6.52.

2-[5-[[2-Methyl-5-(propan-2-yl)phenoxy]methyl]-1,3,4-oxadiazol-2-yl]sulphonyl]-1-(4-(fluorophenyl)ethan-1-one (**3d**): It was obtained as white solid. HPLC t_R (min): 18.44, M.p: 101-103 °C, TLC R_f: 0.60(S3), yield 62%. IR cm⁻¹: 1672 (C=O), 1589 (C=N str), 1120 (C-O-C), 695 (C-S-C). ¹H NMR (300 MHz, DMSO-d₆): δ: 1.18 (d, 6H, J=6.9 Hz, -CH(CH₃)₂); 2.08 (s, 3H, Ar-CH₃); 2.77-2.87 (m, 1H, -CH(CH₃)₂); 5.12 (s, 2H, -S-CH₂-); 5.37 (s, 2H, -O-CH₂-); 6.78 (d, 1H, J=7.5 Hz, Ar-H); 7.05 (d, 1H, J=7.8 Hz, Ar-H); 7.40 (t, 2H, J=7.8 Hz, Ar-H); 8.13 (dd, 2H, J=7.5 Hz, J=2.1 Hz, Ar-H). LR-MS (m/z): calculated for (M+H)⁺: 401.133, found: 401, calculated for (M-H)⁻: 399.118, found: 399. Anal. Calcd. for C₂₁H₂₁FN₂O₃S: C, 62.98; H, 5.29; N, 7.00; S, 8.01. Found: C, 62.16; H, 5.10; N, 6.86; S, 7.83.

2-[5-[[2-Methyl-5-(propan-2-yl)phenoxy]methyl]-1,3,4-oxadiazol-2-yl]sulphonyl]-1-(4-methoxyphenyl)ethan-1-one (**3e**): It was obtained as white solid. HPLC t_R (min): 17.88, M.p: 86-88 °C, TLC R_f: 0.61(S3), yield 74%. IR cm⁻¹: 3110 and 3050 (Ar C-H str), 1658 (C=O), 1595 (C=N str), 1201 (C-O-C), 692 (C-S-C). ¹H NMR (300 MHz, DMSO-d₆): δ: 1.17 (d, 6H, J=6.9 Hz, -CH(CH₃)₂); 2.07 (s, 3H, Ar-CH₃); 2.77-2.87 (m, 1H, -CH(CH₃)₂); 3.34 (s, 3H, -OCH₃); 5.07 (s, 2H, -S-CH₂-); 5.37 (s, 2H, -O-CH₂-); 6.77 (d, 1H, J=7.5 Hz, Ar-H); 6.97 (s, 1H, Ar-H); 7.05 (d, 1H, J=7.8 Hz, Ar-H); 7.10 (dd, 2H, J=8.7 Hz, J=2.1 Hz, Ar-H); 8.01 (dd, 2H, J=8.9 Hz, J=2.1 Hz, Ar-H). LR-MS (m/z): calculated for (M+H)⁺: 413.153, found: 413, calculated for (M-H)⁻: 411.138, found: 411. Anal. Calcd. for C₂₂H₂₄N₂O₄S: C, 64.06; H, 5.86; N, 6.79; S, 7.77. Found: C, 63.61; H, 5.82; N, 6.83; S, 7.62.

2-[5-[[2-Methyl-5-(propan-2-yl)phenoxy]methyl]-1,3,4-oxadiazol-2-yl]sulphonyl]-1-(4-bromine)ethan-1-one (**3f**): It was obtained as white solid. HPLC t_R (min): 26.65, M.p: 111-113 °C, TLC R_f: 0.77(S3), yield 37%. IR cm⁻¹: 3097 and 3014 (Ar C-H str), 1674 (C=O), 1581 (C=N str), 1128 (C-O-C), 707 (C-S-C). ¹H NMR (300 MHz, DMSO-d₆): δ: 1.17 (d, 6H, J=6.9 Hz, -CH(CH₃)₂); 2.07 (s, 3H, Ar-CH₃); 2.77-2.87 (m, 1H, -CH(CH₃)₂); 5.11 (s, 2H, -S-CH₂-); 5.37 (s, 2H, -O-CH₂-); 6.78 (d, 1H, J=7.5 Hz, Ar-H); 6.96 (s, 1H, Ar-H); 7.05 (d, 1H, J=7.5 Hz, Ar-H); 7.80 (dd, 2H, J=8.7 Hz, J=2.1 Hz, Ar-H); 7.97 (dd, 2H, J=8.7 Hz, J=2.1 Hz, Ar-H). LR-MS (m/z): calculated for (M+H)⁺: 461.053, found: 461, calculated for (M-H)⁻: 459.038, found: 459. Anal. Calcd. for C₂₁H₂₁BrN₂O₃S. ½ H₂O: C, 53.62; H, 4.71; N, 5.96; S, 6.82. Found: C, 53.64; H, 4.46; N, 6.05; S, 6.84.

5.3. Molecular modelling studies

Compounds **3a-f** were sketched and prepared according to “prepare ligands” protocol provided in BIOVIA Discovery Studio 4.5 [65]. Molecular docking was based on the crystal structures of COX-1 (PDB ID: 5WBE) [66], COX-2 (PDB ID: 5F19) [67] and mPGES-1 (PDB ID: 5K0I) [68]. Proteins were prepared using “prepare protein” protocol using BIOVIA, where missing loops or residues can be inserted, and hydrogen atoms were added. Docking study was performed using AutoDock4.2. All molecules were allowed to dock for twenty runs into their respective active site. Docking study was performed according to Lamarckian Genetic algorithm using 20 million energy evaluation.

5.4. Biological assays

5.4.1. Cell culture studies

Human cervical cancer cell line (HeLa), human breast cancer cell line (MCF-7), human prostate cancer cell line (PC-3), human lung cancer cell line (A549), human chronic myeloid leukemia cell line (K562) and non-tumorigenic mouse embryonic fibroblast cell line (NIH3T3) were purchased from American Type Culture Collection (ATCC) (Manassas, VA, USA). Cells were cultured in Dulbecco's modified eagle medium (DMEM) (Gibco, Rockville, MD, USA) containing 10% fetal bovine serum (FBS) (Gibco, Rockville, MD, USA) and maintained in a 37°C, 5% CO₂ incubator. Cell passage was conducted at 80-90% confluence.

5.4.2. Cell viability assay

Cell viability was determined by the 3-(4,5-dimethylthiazol-2-yl)-2,5-diphenyltetrazolium bromide (MTT) assay. Briefly, the cells (1×10^4 cells/well) were seeded onto 96-well plates and incubated overnight. Then, the cells were treated with 10 μ M of compounds for 48 h. After the incubation period, MTT was added into each well to a final concentration of 0.5 mg/mL and incubated for 4 h. The culture medium was then removed and 100 μ L of the SDS buffer was added to solubilize the purple formazan product. Absorbances at wavelengths of 570 and 630 nm were measured by a microplate reader (Biotek, Winooski, VT, USA).

5.4.3. mPGES-1 inhibition assays

Preparation of mPGES-1 enzymes

The cloning of mPGES-1 enzyme and the preparation of protein followed the same protocols as described in our previous reports [69]. Briefly, FreeStyle Max Expression system was used to express wild-type human mPGES-1 enzymes. FreeStyle 293-F cells were cultured following manufacturer's manual in FreeStyle 293 expression medium on orbit rotate shaker in 8% CO₂ incubator at 37 °C. Cells were transfected with 1.5 μ g/mL of mPGES-1/pcDNA3 construct using FreeStyle Max reagent at a cell density of 1×10^6 for two days. Transfected cells were collected, washed, and sonicated in TSES buffer (15 mM Tris-HCl, pH 8.0 plus 0.25 M sucrose, 0.1 mM EDTA and 1 mM DTT) on ice. The broken cells were first centrifuged at 12,500 \times g for 10 min. The supernatant was further centrifuged at 105,000 \times g for 1 h at 4 °C. The residual pellet was washed and homogenized in PBS buffer. The crude microsomal mPGES-1 was aliquoted and stored at -80 °C before use.

Activity assay using a recombinant mPGES-1.

The enzyme activity assay was performed using the same protocol as described in our previous reports [45, 70-72]. Briefly, the mPGES-1-catalyzed reaction was performed in 1.5 mL microcentrifuge tubes with reaction mixture of 0.2 Na₂HPO₄/NaH₂PO₄, pH 7.2 (10 μ L); 2.5 mM GSH (2.5 μ L); diluted microsomal human mPGES-1 enzyme (80 μ g/mL, 1 μ L); inhibitor in DMSO solution (1 μ L); 0.31 mM PGH₂ in DMF (5 μ L) and distilled deionized water in a final volume of 100 μ L. An inhibitor was incubated with the enzyme for 15 min at ambient temperature followed by the addition of substrate PGH₂ (stored in dry ice). The enzymatic reaction was started immediately upon the addition of PGH₂. After 1 min of reaction, solution (40 mg/mL SnCl₂ in absolute ethanol, 10 μ L) was added to cease the reaction by converting excess PGH₂ to PGF_{2 α} . The produced PGE₂ from the enzymatic reaction was quantified by the PGE₂ enzyme immunoassay as described earlier [73].

5.4.4. COX-1/2 inhibition assays

The inhibitory potential of all synthesized compounds on COX-1 and COX-2 enzymes were evaluated using a colorimetric COX Inhibitor Screening Kit (Cayman Chemical, Ann Arbor, MI, USA). The samples and control were dissolved in the DMSO and diluted with the reaction buffer to their final concentrations. DMSO served as a negative control for 100% initial activity. We have also tested for inhibitor interference by adding the inhibitor to a boiled enzyme sample as a control. The assay was conducted in duplicate.

* This research was partly presented at the 2nd International Gazi Pharma Symposium Series (GPSS 2017), 11-13 October 2017, Ankara, Turkey.

Acknowledgements: This study was supported by Marmara University Scientific Research Projects Commission under the grant no: SAG-C-DRP-081117-0616.

Author contributions: Concept - İ.K.; Design - İ.K., G.E.; Supervision - İ.K., C.-G.Z., K.Y., Ö.B.Ö.; Resources - İ.K., C.-G.Z., K.Y., Ö.B.Ö.; Materials - İ.K., C.-G.Z., K.Y., Ö.B.Ö.; Data Collection and/or Processing - G.E., K.D., A.E., M.D., Ö.B.Ö.; Analysis and/or Interpretation - G.E., K.D., C.-G.Z., A.E., K.Y., M.D., Ö.B.Ö., İ.K.; Literature Search - G.E., C.-G.Z., K.Y., Ö.B.Ö., İ.K.; Writing - G.E., C.-G.Z., K.Y., Ö.B.Ö., İ.K.; Critical Reviews - G.E., K.D., C.-G.Z., A.E., K.Y., M.D., Ö.B.Ö., İ.K.

Conflict of interest statement: The authors declared no conflict of interest.

REFERENCES

- [1] Basile L, Álvarez S, Blanco A, Santagati A, Granata G, Di Pietro P, Guccione S, Muñoz-Fernández MA. Sulfonilamidothiopyrimidone and thiopyrimidone derivatives as selective COX-2 inhibitors: Synthesis, biological evaluation and docking studies. *Eur J Med Chem.* 2012; 57(0): 149-161. [\[CrossRef\]](#)
- [2] Charlier C, Michaux C. Dual inhibition of cyclooxygenase-2 (COX-2) and 5-lipoxygenase (5-LOX) as a new strategy to provide safer non-steroidal anti-inflammatory drugs. *Eur J Med Chem.* 2003; 38(7-8): 645-659. [\[CrossRef\]](#)
- [3] Dannhardt G, Kiefer W. Cyclooxygenase Inhibitors-Current Status and Future Prospects. *Eur J Med Chem.* 2001; 36: 109-126. [\[CrossRef\]](#)
- [4] Samuelsson B, Morgenstern R, Jakobsson PJ. Membrane prostaglandin E synthase-1: A novel therapeutic target. *Pharmacol Rev.* 2007; 59: 207-224. [\[CrossRef\]](#)
- [5] Akasaka H, So SP, Ruan KH. Relationship of the topological distances and activities between mPGES-1 and COX-2 versus COX-1: implications of the different post-translational endoplasmic reticulum organizations of COX-1 and COX-2. *Biochemistry.* 2015; 54: 3707-3715. [\[CrossRef\]](#)
- [6] Whittle BJR. Gastrointestinal effects of nonsteroidal anti-inflammatory drugs. *Fund Clin Pharmacol.* 2003; 17(3): 301-313. [\[CrossRef\]](#)
- [7] Laine L. The gastrointestinal effects of nonselective NSAIDs and COX-2 selective inhibitors. *Semin Arthritis Rheum.* 2002; 32(3): 25-32. [\[CrossRef\]](#)
- [8] Chang HH, Meuillet EJ. Identification and development of mPGES-1 inhibitors: where are we at? *Future Med Chem.* 2011; 3(15): 1909-1934. [\[CrossRef\]](#)
- [9] Bülbül B, Küçükgülzel I. Microsomal prostaglandin E2 synthase-1 as a new macromolecular drug target in the prevention of inflammation and cancer. *Anti-Cancer Agents Med Chem.* 2019; 19(10): 1205-1222. [\[CrossRef\]](#)
- [10] Kadi AA, El-Brollosy NR, Al-Deeb OA, Habib EE, Ibrahim TM, El-Emam AA. Synthesis, antimicrobial and anti-inflammatory activities of novel 2-(1-adamantyl)-5-substituted-1,3,4-oxadiazoles and 2-(1-adamantylamino)-5-substituted-1,3,4-thiadiazoles. *Eur J Med Chem.* 2007; 42: 235-242. [\[CrossRef\]](#)
- [11] Ahsan MJ, Samy JG, Khalilullah MS, Nomani MS, Saraswat P, Gaur R, Singh A. Molecular properties prediction and synthesis of novel 1,3,4-oxadiazole analogues as potent antimicrobial and antitubercular agents. *Bioorg Med Chem Lett.* 2011; 21: 7246-7250. [\[CrossRef\]](#)
- [12] Pinna GA, Murineddu G, Murruzzu C, Zuco V, Zunino F, Cappelletti G, Artali R, Cignarella G, Solano L, Villa S. Synthesis, modelling and antimetabolic properties of tricyclic systems characterized by a 2-(5-phenyl-1-H-pyrrol-3-yl)-1,3,4-oxadiazole moiety. *ChemMedChem.* 2009; 4: 998-1009. [\[CrossRef\]](#)
- [13] Zhang XM, Qui M, Sun J, Zhang YB, Yang YS, Wang XL, Zhu HL. Synthesis, biological evaluation and molecular docking studies of 1,3,4-oxadiazole derivatives possessing 1,4-benzodioxan moiety as potential anticancer agents. *Bioorg Med Chem.* 2011; 19: 6518-6524. [\[CrossRef\]](#)
- [14] Du QR, Li DD, Pi YZ, Li JR, Sun J, Fang F, Zhong WQ, Gong HB, Zhu HL. Novel 1,3,4-oxadiazole thioether derivatives targeting thymidylate synthase as dual anticancer/antimicrobial agents. *Bioorg Med Chem.* 2013; 21: 2286-2297. [\[CrossRef\]](#)
- [15] Bajaj S, Roy PP, Singh J. Synthesis, thymidine phosphorylase inhibitory and computational study of novel 1,3,4-oxadiazole-2-thione derivatives as a potential anticancer agents. *Comput Biol Chem.* 2018; 74: 151-160. [\[CrossRef\]](#)
- [16] Kulabaş N, Tatar E, Özakpınar ÖB, Özsvacı D, Pannecouque C, De Clercq E, Küçükgülzel İ. Synthesis and antiproliferative evaluation of novel 2-(4H-1,2,4-triazole-3-ylthio)acetamide derivatives as inducers of apoptosis in cancer cells. *Eur J Med Chem.* 2016; 121: 58-70. [\[CrossRef\]](#)
- [17] Gahani U, Ullah N. New potent inhibitors of tyrosinase: Novel clues to binding of 1,3,4-thiadiazole-2(3H)-thiones, 1,3,4-oxadiazole-2(3H)-thiones, 4-amino-1,2,4-triazole-5(4H)-thiones, and substituted hydrazides to the dicopper active site. *Bioorg Med Chem.* 2010; 18(11): 4042-4048. [\[CrossRef\]](#)
- [18] Zhang LR, Liu ZJ, Zhang H, Sun J, Luo Y, Zhao TT, Gong HB, Zhu HL. Synthesis, biological evaluation and molecular docking studies of novel 2-(1,3,4-oxadiazol-2-ylthio)-1-phenylethanone derivatives. *Bioorg Med Chem.* 2012; 20: 3615-3621. [\[CrossRef\]](#)
- [19] Zhang S, Luo Y, He LQ, Liu ZJ, Jiang AQ, Yang YH, Zhu HL. Synthesis, biological evaluation and molecular docking studies of novel 1,3,4-oxadiazole derivatives possessing benzotriazole moiety as FAK inhibitors with anticancer activity. *Bioorg Med Chem.* 2013; 21: 3723-3729. [\[CrossRef\]](#)
- [20] Yurttaş L, Bülbül EF, Tekinkoca S, Demirayak Ş. Antimicrobial activity evaluation of new 1,3,4-oxadiazole derivatives. *Acta Pharm Sci.* 2017; 55(2): 45-54. [\[CrossRef\]](#)

- [21] He S, Li C, Liu Y, Lai L. Discovery of highly potent microsomal prostaglandin E2 synthase-1 inhibitors using the active conformation structural model and virtual screen. *J Med Chem*. 2013; 56: 3296-3309. [CrossRef]
- [22] Abd-Ellah SH, Abdel-Aziz M, Shoman ME, Beshr EAM, Kaoud TS, Ahmed ASFF. New 1,3,4-oxadiazole/oxime hybrids: Design, synthesis, anti-inflammatory, COX inhibitory and ulcerogenic liability. *Bioorg Chem*. 2017; 74: 15-29. [CrossRef]
- [23] Wu W, Chen Q, Tai A, Jiang G, Ouyang G. Synthesis and antiviral activity of 2-substitutedmethylthio-5-(4-amino-2-methylpyrimidin-5-yl)-1,3,4-oxadiazole derivatives. *Bioorg Med Chem Lett*. 2015; 25: 2243-2246. [CrossRef]
- [24] Kordali S, Cakir A, Ozer H, Ckamakçı R, Kesdek M, Mete E. Antifungal, phytotoxic and insecticidal properteis of essential oil isolated Turkish *Orifanum acutidens* and its three components carvacrol, thymol and p-cymene. *Biosource Tech*. 2008; 99: 8788-8795. [CrossRef]
- [25] Guarda A, Rubilar JF, Miltz J, Galotto MJ. The antimicrobial activity of microencapsulated thymol and carvacrol. *J Food Microbiol*. 2011; 146: 144-150. [CrossRef]
- [26] Ghomi JS, Ebrahimabadi AH, Bidgoli ZD, Batooli H. GC/MS analysis and in vitro antioxidant activity of essential oil and methanol extracts of *Thymus caramicus* jasals and its main constituent carvacrol. *Food Chem*. 2009; 115: 1524-1528. [CrossRef]
- [27] Yin QH, Yan FX, Zu XY, Wu YH, Wu XP, Liao MC, Deng SW, Yin LI, Zhuang YZ. Anti-proliferative and pro-apoptotic effect of carvacrol on human hepatocellular carcinoma cell line HepG-2. *Cytotechnology*. 2012; 64: 43-51. [CrossRef]
- [28] Fan K, Xiaolei L, Cao Y, Qi H, Li L, Zhang Q, Sun H. Carvacrol inhibits proliferation and induces apoptosis in human colon cancer cells. *Anti-Cancer Drugs*. 2015; 26(8): 813-823. [CrossRef]
- [29] Günes-Bayır A, Kızıltan HS, Kocyyigit A, Güler EM, Karatas E, Toprak A. Effects of natural phenolic compound carvacrol on the human gastric adenocarcinoma (AGS) cells in vitro. *Anti-Cancer Drugs*. 2017; 28: 522-530. [CrossRef]
- [30] Wagner H, Wierer M, Bauer R. In vitro inhibition of prostaglandin biosynthesis by essential oils and phenolic compounds. *Planta Med*. 1986; 52: 184-187.
- [31] Landa P, Kokoska L, Pribylova M, Vanek T, Marsik P. In vitro anti-inflammatory activity of carvacrol: Inhibitory effect on COX-2 catalyzed prostaglandin E2 biosynthesis. *Arch Pharm Res* 2009; 32: 75-78. [CrossRef]
- [32] Lima MDS, Quintans-Junior L, Santana WAD, Kaneto CM, Soaers MBP, Villareal CF. Anti-inflammatory effects of carvacrol: Evidence for a key role of interleukin-10. *Eur J Pharm*. 2013; 699: 112-117. [CrossRef]
- [33] Riendeau D, Aspiotis R, Ethier D, Gareau Y, Grimm EL, Guay J, Guiral S, Juteau H, Mancini JA, Methot N, Rubin J, Friesen RW. Inhibitors of the inducible microsomal prostaglandin E2 synthase (mPGES-1) derived from MK-886. *Bioorg Med Chem Lett*. 2005; 15: 3352-3355. [CrossRef]
- [34] Cote B, Boulet L, Brideau C, Claveau D, Ethier D, Frenette R, Gagnon M, Giroux A, Guay J, Guiral S, Mancini J, Martins E, Masse F, Methot N, Riendeau D, Rubin J, Xu D, Yu H, Ducharme Y, Friesen RW. Substituted phenanthrene imidazoles as potent, selective, and orally active mPGES-1 inhibitors. *Bioorg Med Chem Lett*. 2007; 17: 6816-6820. [CrossRef]
- [35] Wu YC, Su LJ, Wang HW, Lin CFJ, Hsu WH, Chou TY, Huang CFY, Lu CL, Hsueh CT. Co-Overexpression of Cyclooxygenase-2 and microsomal prostaglandin E synthase-1 adversely affects the prospective survival in non-small cell lung cancer. *J Thorac Oncol*. 2010; 5(8): 1167-1174. [CrossRef]
- [36] Chiasson JF, Boulet L, Brideau C, Chau A, Claveau D, Cote B, Ethier D, Giroux A, Guay J, Guiral S, Mancini J, Masse F, Methot N, Riendeau D, Roy P, Rubin J, Xu D, Yu H, Ducharme Y, Friesen RW. Trisubstituted ureas as potent and selective mPGES-1 inhibitors. *Bioorg Med Chem Lett*. 2011; 21: 1488-1492. [CrossRef]
- [37] Shiro T, Takahashi H, Kakiguchi K, Inoue Y, Masuda K, Nagata H, Tobe M. Synthesis and SAR study of imidazoquinolines as a novel structural class of microsomal prostaglandin E2 synthase-1 inhibitors. *Bioorg Med Chem Lett*. 2012; 22: 285-288. [CrossRef]
- [38] Shiro T, Kakiguchi K, Takahashi H, Nagata H, Tobe M. Synthesis and biological evaluation of substituted imidazoquinoline derivatives as mPGES-1 inhibitors. *Bioorg. Med Chem*. 2013; 21: 2068-2078. [CrossRef]
- [39] Shiro T, Kakiguchi K, Takahashi H, Nagata H, Tobe M. 7-Phenyl-imidazoquinolin-4(5H)-one derivatives as selective and orally available mPGES-1 inhibitors. *Bioorg Med Chem*. 2013; 21: 2868-2878. [CrossRef]
- [40] Lauro G, Tortorella P, Bertamino A, Ostacolo C, Koerle A, Fischer K, Brun I, Terracciano S, Monterrey IMG, Tauro M, Loiodice F, Novellino E, Riccio R, Werz O, Campiglia P, Bifulco G. Structure-based design of microsomal prostaglandin E2 synthase (mPGES-1) inhibitors using a virtual fragment growing optimization scheme. *ChemMedChem*. 2016; 11: 612-619. [CrossRef]

- [41] Larsson K, Jakobsson PJ. Inhibition of microsomal prostaglandin E synthase-1 as targeted therapy in cancer treatment. *Prostag Oth Lip M*. 2015; 120: 161-165. [CrossRef]
- [42] Koeberle A, Laufer SA, Werz O. Design and development of microsomal prostaglandin E2 synthase-1 inhibitors: challenges and future directions. *J Med Chem*. 2016; 59: 5970-5986. [CrossRef]
- [43] Jin Y, Smith CL, Hu L, Campanale KM, Stoltz R Huffman Jr LG, McNearney TA, Yang XY, Ackermann BL, Dean R, Regev A, Landschulz W. Pharmacodynamic comparison of LY3023703, a novel microsomal prostaglandin synthase 1 inhibitor, with celecoxib. *Clin Pharmacol Ther*. 2016; 99: 274-284. [CrossRef]
- [44] Sant S, Tandon M, Menon V, Gudi G, Kattige V, Joshi NK, Korukonda K, Dolberg OL. GRC 27864, novel, microsomal prostaglandin E synthase-1 enzyme inhibitor: phase 1 study to evaluate safety, PK and biomarkers in healthy, adult subjects. *Osteoarthr Cartilage*. 2018; 26(1): 351-352. [CrossRef]
- [45] Ding K, Zhou Z, Hou S, Yuan Y, Zhou S, Zheng J, Chen C, Loftin C, Zheng F, Zhan CG. Structure-based discovery of mPGES-1 inhibitors suitable for preclinical testing in wild-type mice as a new generation of anti-inflammatory drugs. *Sci Rep*. 2018; 8: 5205. [CrossRef]
- [46] Waltenberger B, Wiechmann K, Bauer J, Markt P, Noha SM, Wolber G, Rollinger JM, Werz O, Schuster D, Stuppner H. Pharmacophore modelling and virtual screening for novel acidic inhibitors of microsomal prostaglandin E2 synthase-1 (mPGES-1). *J Med Chem*. 2011; 54: 3163-3174. [CrossRef]
- [47] Bergqvist F, Ossiápvva E, Weway K, Idprg H, Checa A, Englund K, Englund P, Khoonsari PE, Kultima K, Wheelock CE, Larsson K, Korotkova M, Jakobsson PJ. Inhibition of mPGES-1 or COX-2 results in different proteomic and lipidomic profiles in A549 lung cancer cells. *Front Pharmacol*. 2019; 10: 636. [CrossRef]
- [48] Gür ZT, Çalışkan B, Garscha U, Olguç A, Schubert US, Gerstmeier J, Werz O, Banoğlu E. Identification of multi-target inhibitors of leukotriene and prostaglandin E2 biosynthesis by structural tuning of the FLAP inhibitor BRP-7. *Eur J Med Chem*. 2018; 150: 876-899. [CrossRef]
- [49] Bagul SD, Rajput JD, Tadavi SK, Bendre RS. Design, synthesis and biological activities of novel 5-isopropyl-2-methylphenolhydrazone-based sulfonamide derivatives. *Res Chem Intermed*. 2016; 43(4): 2241-2252. [CrossRef]
- [50] Lacasse G, Muchowski JM. Five-Membered Heterocyclic Thions. Part II. Oxadiazole-2-thione. *Can J Chem*. 1972; 50: 3082-3083.
- [51] Öztürk S, Akkurt M, Cansız A, Çetin A, Şekerci M, Heinemann FW. 5-(Furan-2-yl)-1,3,4-oxadiazole-2(3H)-thione. *Acta Crystallogr B*. 2004; E60: o322-o323. [CrossRef]
- [52] Horning DE, Muchowski JM. Five-membered heterocyclic thiones. Part I. 1,3,4-oxadiazole-2-thione. *Canadian J Chem*. 1972; 50: 3079.
- [53] Tomi IHR, Al-Qaisi AHJ, Al-Qaisi ZHJ. Synthesis, characterization and effect of bis 1,3,4-oxadiazole containing glycine moiety on the activity of some transferase enzymes. *J King Saud Univ Sci*. 2011; 23(3): 23-33. [CrossRef]
- [54] Gürsoy A, Demirayak Ş, Cesur Z, Reisch J, Ötük G. Synthesis of some new hydrazide-hydrazones, thiosemicarbazides, thiadiazoles, triazoles and their derivatives as possible antimicrobials. *Pharmazie*. 1990; 21(42): 246-250. [CrossRef]
- [55] Hamza A, Zhao X, Tong M, Tong M, Tai HH, Zhan CG. Novel human mPGES-1 inhibitors identified through structure-based virtual screening. *Bioorg Med Chem*. 2011; 19(20): 6077-6086. [CrossRef]
- [56] Dhanjal JK, Sreenidhi AK, Bafna K, Katiyar SP, Goyal S, Grover A, Sundar D. Computational structure-based *de novo* design of hypothetical inhibitors against the anti-inflammatory target COX-2. *PLoS ONE*. 2015; 10(8), e0134691. [CrossRef]
- [57] Morris GM, Ruth H, Lindstrom W, Sanner MF, Belew RK, Goodsell DS, Olson AJ. Software news and updates AutoDock4 and AutoDockTools4: Automated docking with selective receptor flexibility. *J Comp Chem*. 2009; 30(16): 2785-2791. [CrossRef]
- [58] SwissADME, <http://www.swissadme.ch/> (accessed on 29 Jan 2020).
- [59] Zhao YH, Abraham MH, Le J, Hersey A, Luscombe CN, Beck G, Sherbone B, Cooper I. Rate-limited steps of human oral absorption and QSAR studies. *Pharm Res*. 2002; 19(10): 1446-1457. [CrossRef]
- [60] Fromm MF. P-glycoprotein: A defense mechanism limiting oral bioavailability and CNS accumulation of drugs. *Int J Clin Pharmacol Ther* 2000; 38: 69-74. [CrossRef]
- [61] Kaplan YC, Gelal A. The role of p-glycoprotein in pharmacokinetics and toxicokinetic. *Turkiye Klinikleri J Surg Med Sci*. 2006; 2(46): 33-38.
- [62] Daina A, Zoete V. A BOILED-Egg to predict gastrointestinal absorption and brain penetration of small molecules. *ChemMedChem*. 2016; 11(11): 1117-1121. [CrossRef]

- [63] ACD Labs, <https://www.acdlabs.com/index.php> (accessed on 29 Jan 2020).
- [64] Manjunatha K, Poojary B, Lobo PL, Fernandes J, Kumari NS. Synthesis and biological evaluation of some 1,3,4-oxadiazole derivatives. *Eur J Med Chem.* 2010; 45: 5225-5233. [CrossRef]
- [65] Dassault Systèmes BIOVIA Discovery Studio 2017 R2: A comprehensive predictive science application for the Life Sciences. San Diego, CA, USA. (2017).
- [66] Cingolani G, Panella A, Perrone MG, Vitale P, Di Mauro G, Fortuna CG, Armen RE, Ferorelli S, Smith WL, Scilimati A. Structural basis for selective inhibition of cyclooxygenase-1 (COX-1) by diarylisoxazoles mofezolac and 3-(5-chlorofuran-2-yl)-5-methyl-4-phenylisoxazole. *Eur J Med Chem.* 2017; 138: 661-668. [CrossRef]
- [67] Lucido MJ, Orlando BJ, Vecchio AJ, Malkowski MG. Crystal structure of aspirin-acetylated human Cyclooxygenase-2: Insight into the formation of products with reversed stereochemistry. *Biochemistry.* 2016; 55(8): 1226-1238. [CrossRef]
- [68] Kuklish SL, Antonysamy S, Bhattachar SN, Chandrasekhar S, Fisher MJ, Fretland AJ, Gooding K, Harvey A, Hugnes NE, Luz JG, Manninen PR, McGee JE, Navarro A, Norman BH, Prtridge KM, Quimby SJ, Schiffler MA, Sloan AV, Warshawsky AM, York JS, Yu XP. Characterization of 3,3-dimethyl substituted N-aryl piperidines as potent microsomal prostaglandin E synthase-1 inhibitors. *Bioorg Med Chem Lett.* 2016; 26(19): 4824-4828. [CrossRef]
- [69] Hamza A, Tong M, Abdulhameed MDM, Liu J, Goren AC, Tai HH, Zhan CG. Understanding microscopic binding of human microsomal prostaglandin E synthase-1 (mPGES-1) trimer with substrate PGH₂ and cofactor GSH: Insights from computational alanine scanning and site-directed mutagenesis. *J Phys Chem B.* 2010; 114: 5605-5616. [CrossRef]
- [70] Ding K, Zhou Z, Zhou S, Yuan X, Kim K, Zhang T, Zheng X, Zheng F, Zhan CG. Design, synthesis and discovery of 5-((1,3-diphenyl-1*H*-pyrazol-4-yl)methylene)pyrimidine-2,4,6(1*H*,3*H*,5*H*)-triones and related derivatives as novel inhibitors of mPGES-1. *Bioorg Med Chem Lett.* 2018; 27: 858-862. [CrossRef]
- [71] Hamza A, Zhao X, Tong M, Tai HH, Zhan CG. Bioorg Med Chem. Novel human mPGES-1 inhibitors identified through structure-based virtual screening. *Bioorg Med Chem.* 2011; 19: 6077-6086. [CrossRef]
- [72] Zhou Z, Yuan Y, Zhou S, Ding K, Zheng F, Zhan CG. Selective inhibitors of human mPGES-1 from structure-based computational screening. *Bioorg Med Chem Lett.* 2017; 27: 3739-3743. [CrossRef]
- [73] Harding L, Wang Z, Tai HH. Stimulation of prostaglandin E2 synthesis by interleukin-1 β is amplified by interferons but inhibited by interleukin-4 in human amnion-derived WISH cells. *Biochim Biophys Acta.* 1996; 1310: 48-52. [CrossRef]

This is an open access article which is publicly available on our journal's website under Institutional Repository at <http://dspace.marmara.edu.tr>.